WATER RESOURCES RESEARCH, VOL. 32, NO. 5, PAGES 1429–1439, MAY 1996

Self-affinity in braided rivers

Victor Sapozhnikov and Efi Foufoula-Georgiou
St. Anthony Falls Laboratory, University of Minnesota, Minneapolis

Abstract. Three braided rivers of different scales and different hydrologic/geomorphologic characteristics (the Aichilik and Hulahula in Alaska and the Brahmaputra in Bangladesh) are analyzed for spatial scaling using a logarithmic correlation integral method developed earlier by the authors. It is shown that the rivers exhibit anisotropic scaling (self-affinity) with fractal exponents $\nu_x = 0.72–0.74$ and $\nu_y = 0.51–0.52$, the x axis being oriented along the river and the y axis in the perpendicular direction. The fact that despite large differences in scales (0.5–15 km in braid plain width), slopes (7×10^{-3} to 8×10^{-5}), and types of bed material (gravel to sand), the analyzed braided rivers show similar spatial scaling deserves special attention. It might indicate the presence of universal features in the underlying mechanisms responsible for the formation of the spatial structure of braided rivers. Also, comparison of fractal characteristics of braided rivers with those of single-channel rivers and river networks suggests that braided rivers form a class of fractal objects lying between the classes of single-channel rivers and river networks.

1. Introduction

Braided rivers, i.e., rivers "having a number of alluvial channels with bars and islands between meeting and dividing again" [*Lane*, 1957], form a separate class of hydrologic systems, other than single-channel rivers and river networks. They prevail in mountainous and glacial regions and are highly dynamic systems characterized by intensive erosion, sediment transport and deposition, and frequent channel shifting. Study of the morphology of the braided rivers and processes governing their behavior is important in geomorphology, geology, hydrology, and environmental studies. The alluvial deposits of braided rivers are important reservoirs of water, oil, gas, coal, sand, gravel, and heavy minerals. Despite their importance, braided rivers have not been studied as extensively as single-channel rivers and river networks (see, for example, *Bristow and Best* [1993]). In particular, there is a significant lack of quantitative studies in braided rivers; the existing models and frameworks are mostly qualitative. With the exception of the early work by *Howard et al.* [1970] it is only recently that some more quantitative studies were carried out, such as, for example, that of *Murray and Paola* [1994, 1996], *Murray* [1995], and *Webb* [1995].

Braided rivers exist over a large range of scales from several meters to 20 km in width. It is clear that when applying results from one braided river to another of different size, or from a physical model to a real braided river, the issue of scale and its effect on the geometry, runoff, and forming processes of the river inevitably arises. Scale relationships are also important in understanding the internal structure of a particular braided river. Indeed, the processes shaping a braided river and causing branching, confluence and bar growth, and erosion act over a wide range of scales and produce an internal structure which also manifests itself over a large range of scales. Exploring scale relations in the internal structure of braided rivers can help to understand better the processes responsible for sculpturing the river. To address these questions, quantitative tools for the description of the geometric and hydrologic characteristics of braided rivers are needed.

Paper number 96WR00490.
0043-1397/96/96WR-00490$09.00

In braided rivers, sinuosity of individual channels and their branching and confluence produces a rather complex and hierarchical spatial structure which needs appropriate tools for its description. Often, such complex structures find their natural description in terms of self-similar or self-affine fractals [*Mandelbrot*, 1982]. At first glance the spatial structure of the whole braided river and its structure at the level of channels appear to have some kind of similarity [see *Bristow and Best*, 1993]. This impression, however, needs to be either validated or disproved by quantitative analysis.

The presence of scaling in a phenomenon means that statistical properties of the phenomenon at one scale relate to its statistical properties at another scale via a transformation which involves only the ratio of the two scales. This implies a certain invariance of the phenomenon under magnification or contraction (scale invariance). Objects showing the same spatial scaling in all directions (which makes it impossible to determine the scale of the object from its photograph) are called self-similar fractals and can be characterized by their fractal dimension D. In a more general case, scaling properties are different in different directions. Such anisotropically scaled objects are called self-affine fractals and are characterized by more than one fractal exponents which properly reflect scaling in each direction. In terms of fractal dimension a self-affine fractal is characterized not by one but rather by two fractal dimensions: the local fractal dimension D_L and the global fractal dimension D_G [*Mandelbrot*, 1986].

Spatial scaling has been established for single-channel rivers and river networks [see *Tarboton et al.*, 1988; *La Barbera and Rosso*, 1989; *Nikora*, 1991; *Sapozhnikov and Nikora*, 1993; *Peckham*, 1995]. Moreover, it was shown that the fractal geometry of river networks is closely connected to other hydrologic characteristics, such as distribution of discharge masses and of energy dissipation in river basins [e.g., *Rodriguez-Iturbe et al.*, 1992]. *Nikora et al.* [1993] demonstrated that natural and simulated individual streams show a complicated geometry:

self-similarity at small scales and self-affinity at larger scales. Self-affine behavior of the streams is caused by gravity which makes the streams scale differently in the direction of the mainstream slope and in the perpendicular direction. Self-affinity in natural river courses was also reported by *Ijjasz-Vasquez et al.* [1994]. Anisotropic spatial scaling ("external scaling," see section 2) was revealed in simulated river networks [e.g., *Kondoh et al.*, 1987; *Meakin et al.*, 1991]. *Nikora and Sapozhnikov* [1993] found that both natural and simulated river networks show isotropic scaling at small scales and anisotropic scaling at larger scales.

In contrast to a great number of papers existing on fractal properties of rivers and river networks the scaling in braided rivers has virtually not been studied. We are aware only of one study by *Nikora et al.* [1995], who analyzed several sections of New Zealand rivers as self-similar objects and reported fractal dimension $D = 1.5–1.7$. However, the presence of gravity which causes the scaling anisotropy in individual streams and river networks provides reasons to expect self-affine geometry in the braided streams too. The problem is that until recently no method existed for analyzing scaling anisotropy (self-affinity) except for the special case of a nonbranched line [see *Matsushita and Ouchi*, 1989; *Nikora et al.*, 1993] or of an object having a distinct hierarchical structure (e.g., one can easily find fractal exponents for a self-affine Sierpinsky carpet; see also *Nikora and Sapozhnikov* [1993] and *Nikora* [1994], who used scaling of subbasins to estimate fractal exponents of river networks).

It was only recently that a method was developed by the authors to study self-affinity in objects having any topology [*Sapozhnikov and Foufoula-Georgiou*, 1995]. The method is applied in this paper to study the self-affine characteristics of three braided rivers (Brahmaputra in Bangladesh and Aichilik and Hulahula in Alaska). It is found that these rivers exhibit self-affine scaling, the fractal exponents being $\nu_x = 0.72–0.74$ and $\nu_y = 0.51–0.52$. The fact that the fractal exponents ν_x and ν_y are practically the same for all three rivers is worth noticing given that these rivers exist over disparate spatial scales (from 0.5 to 15 km in braid plain widths and from 6.4 to 200 km in length of analyzed sections) and have different slopes (7×10^{-3} to 8×10^{-5}) and different types of bed material (gravel to sand).

This paper is structured as follows. In section 2 the difference between "internal" and "external" fractal exponents is discussed. It is emphasized that the internal fractal exponents (ν_x and ν_y) characterize the internal self-affine structure of a braided river; that is, they show how parts of the whole object scale with respect to each other. These exponents should not be confused with the external self-affine exponents (α_x and α_y) which show how the whole object scales with respect to other (whole) objects and which could be obtained by analyzing a large number of rivers as realizations of an ensemble. Section 3 presents a method for estimating the internal self-affine fractal exponents of an object of any geometry. More details of this method are given by *Sapozhnikov and Foufoula-Georgiou* [1995]. In section 4 the results of the application of this method to three braided rivers are presented. In section 5 we study robustness of the proposed method in estimating the fractal exponents of natural rivers. In section 6, scaling in the sizes of islands in the three studied rivers is analyzed and compared with the results obtained in section 4. Concluding remarks are given in section 7.

2. Internal Versus External Self-Affine Scaling

Each part of a self-affine object is an image of the whole object (either strictly or in a statistical sense) scaled differently in different directions. In other words, if we take a part of the object within a $X \times Y$ rectangle and then change X and Y in a certain different way, we will get the same pattern. This finds its mathematical expression in the relationship

$$M(X, Y) \sim X^{1/\nu_x} \sim Y^{1/\nu_y} \tag{1}$$

where $M(X, Y)$ is the mass of the object within the rectangle of size $X \times Y$ and ν_x and ν_y are the fractal exponents. In the case of self-similarity this equation takes the form

$$M(R) \sim R^D, \tag{2}$$

where $R = X = Y$ is the length of the square side.

While there are several methods for determination of the fractal dimension of self-similar objects, methods for determination of the fractal exponents characterizing self-affine objects seem to be much less developed. The fractal dimension of a self-similar object can be easily estimated from a pattern of the object. However, in a general case, one cannot find the fractal exponents ν_x and ν_y from a pattern of a self-affine object. The problem is that the mass M scales only if the sides of the rectangle change in a certain different way, and in contrast to the self-similar case we do not know a priori how to change X and Y because we do not know the ratio ν_x/ν_y. We can only state that the mass within the rectangle scales provided $X^{1/\nu_x} \sim Y^{1/\nu_y}$.

The methods available for studying a general self-affine object do not analyze the geometry of the object but rather follow how the mass M_0 of the total object changes as the sides X_0 and Y_0 of the object change. If one has available either an ensemble of the same type of objects of different size or patterns of the object at different stages of growth, the ensemble or the evolution of the object can be characterized by exponents α_x and α_y using the relationship

$$M_0(X_0, Y_0) \sim X_0^{1/\alpha_x} \sim Y_0^{1/\alpha_y} \tag{3}$$

We will call α_x and α_y external exponents, in contrast to the internal exponents ν_x and ν_y that characterize the geometry of the object. Since methods for extracting the internal exponents from a pattern of the object are not available in a general case, external exponents instead of internal ones have often been used to describe the geometry of the object [e.g., *Kondoh et al.*, 1987; *Meakin et al.*, 1991]. However, this approach supposes that internal and external exponents are equivalent. *Sapozhnikov and Foufoula-Georgiou* [1995] demonstrated that this supposition is, generally speaking, wrong. To get an idea of the difference between internal and external exponents, let us consider here two examples.

1. Let us consider a trajectory of a biased random walk, such that every jump has a projection on the x axis equal to 1 and a projection on the y axis equal to 1 or -1 with equal probability (e.g., one can think of this trajectory as a simplified representation of a river). This trajectory is known to be a self-affine fractal [e.g., *Mandelbrot*, 1982, p. 350]. Its geometry is characterized by fractal exponents $\nu_x = 1$ (which implies that the average projection X of a part of the trajectory on the x axis depends linearly on its length, measured along the trajectory, or on its "mass" M) and $\nu_y = 1/2$ (implying that the

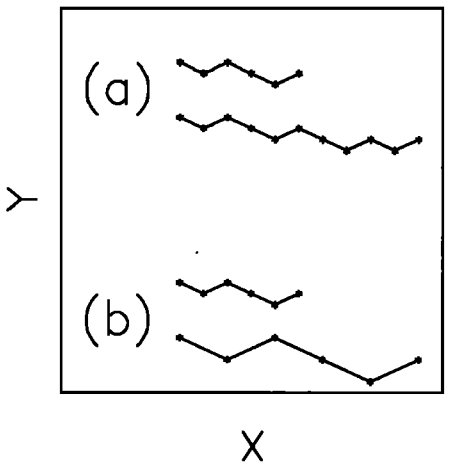

Figure 1. Two types of ensembles of biased random walk trajectories ("rivers") having the same internal fractal exponents $\nu_x = 1$, $\nu_y = 1/2$ but different external exponents α_x and α_y (two elements of each ensemble are shown). (a) The step length of the walk is preserved within the ensemble, which gives $\alpha_x = 1$, $\alpha_y = 1/2$, and (b) the number of steps is preserved within the ensemble, which gives $\alpha_x = 1$, $\alpha_y = 1$.

projection Y of a part of the trajectory on the y axis is proportional to the square root of the length of that part of the trajectory). Suppose now that one has an ensemble of biased random walk trajectories and wants to find its external fractal exponents α_x and α_y, i.e., find the dependence of the projections of the whole trajectory, X_0 and Y_0, on the length of the trajectory M_0. It turns out that the values of the exponents α_x and α_y depend on the way the ensemble is constructed. If the length of the jump is preserved within the ensemble, as shown in Figure 1a (e.g., one can think of rivers having similar hydrologic characteristics and therefore the same sinuosity), then a shorter trajectory is statistically equivalent to a part of same length of the longer trajectory; that is, it has the same projection. Therefore the external exponents of the ensemble α_x and α_y are equal to the internal exponents ν_x and ν_y of each trajectory. However, in another ensemble, shown in Figure 1b, where the trajectories have the same number of jumps but each trajectory has a different jump length (e.g., one can think of rivers having different widths and therefore different characteristic lengths of persistence of the direction of their flows), both projections X_0 and Y_0 of trajectories are obviously proportional to the length of the trajectories, i.e., $\alpha_x = \alpha_y = 1$, different from the internal exponents $\nu_x = 1$ and $\nu_y = 1/2$.

2. In some cases the ensemble of objects is characterized by the external exponents, but the internal exponents of the objects are not defined uniquely at all. As the simplest case, let us consider here compact objects. For example, Scheidegger river networks obtained by computer simulation are shown to be compact objects, and their ensemble is characterized by the values $\alpha_x = 2/3$, $\alpha_y = 1/3$ [*Kondoh et al.*, 1987, p. 1913; *Meakin et al.*, 1991, p. 409]. It is implied (e.g., see discussion after equation (4) of *Kondoh et al.* [1987]) that these exponents characterize the fractal geometry of the networks. However, the compactness of a two-dimensional object means that the object is just a piece of a plane. This, in turn, means that in contrast to the external components α_x and α_y, which characterize the ensemble of the networks, the internal exponents characterizing their geometry are not defined uniquely. For instance, it is quite obvious that a piece of a plane can be treated as a self-similar object as well and can be characterized by $\nu_x = \nu_y = 1/D = 1/2$. The nonuniqueness of the fractal exponents ν_x and ν_y can arise for noncompact objects too. *Sapozhnikov and Foufoula-Georgiou* [1995] showed that a class of noncompact fractal objects exists for which the internal exponents ν_x and ν_y are still not defined uniquely and derived general conditions under which an object falls into this class.

The above examples demonstrate that the external exponents α_x and α_y not only require a set of patterns for their estimation but, generally speaking, are something different from the internal exponents ν_x and ν_y. Therefore *Sapozhnikov and Foufoula-Georgiou* [1995] elaborated a method that enabled extraction of the internal fractal exponents from a pattern of an object of any topology. This method is briefly presented in the next section. The reader is referred to *Sapozhnikov and Foufoula-Georgiou* [1995] for more details and example applications.

3. A Logarithmic Correlation Integral Method for Studying the Geometry of Self-Affine Objects

3.1. Estimation of the Fractal Exponents ν_x and ν_y

Let us write the scaling equation (equation (3)) describing a self-affine object in the form

$$(X_2/X_1)^{1/\nu_x} = (Y_2/Y_1)^{1/\nu_y} = (M_2/M_1). \tag{4}$$

where $M_1 \equiv M(X_1, Y_1)$ is the mass of the object within a rectangle of size $X_1 \times Y_1$ and M_2 is similarly defined. Introducing $x = \log X$, $y = \log Y$, and $z = \log M$, we rewrite the above equation as

$$\frac{x_2 - x_1}{\nu_x} = \frac{y_2 - y_1}{\nu_y} = z_2 - z_1, \tag{5}$$

or

$$(dx/\nu_x) = (dy/\nu_y) = dz. \tag{6}$$

The function $M(X, Y)$ is known as the correlation integral [see *Grassberger and Procaccia*, 1982, p. 191]. Here by analogy we call the function $z(x, y)$ logarithmic correlation integral of the object under study.

Notice from (5) and (6) that $z(x, y)$ is a cylindric surface i.e., a surface that has constant derivative in a specific direction (the direction of the cylinder generating line). The second equality in (6) is true only if the first one is true. Comparing (6) with the generic equation of the differential of the $z(x, y)$ function, that is, $(\partial z/\partial x)\, dx + (\partial z/\partial y)\, dy = dz$, we obtain

$$\nu_x(\partial z/\partial x) + \nu_y(\partial z/\partial y) = 1. \tag{7}$$

The last relationship provides a method for estimating the fractal exponents ν_x and ν_y of a self-affine object. Indeed, having estimated the logarithmic correlation integral $z(x, y)$ from a pattern of the object (by direct calculation of the mass $M(X, Y)$ within rectangles of sizes $X \times Y$), one can calculate the derivatives $\partial z(x, y)/\partial x$ and $\partial z(x, y)/\partial y$ and use them to find the values of ν_x and ν_y that satisfy (7). Ideally, two points (x, y) giving different values of the derivatives $\partial z(x, y)/\partial x$ and $\partial z(x, y)/\partial y$ are sufficient, but for a good estimation it is preferable to compute the derivatives at all (x, y) points and follow a least squares estimation technique. The effectiveness

of this method in estimating the self-affine fractal exponents from single patterns is demonstrated by *Sapozhnikov and Foufoula-Georgiou* [1995] using simulated fractal objects.

3.2. Quantifying the Other Correlation Characteristics of Self-Affine Objects

The solution of (7), as well as of (6), is

$$z(x, y) = \frac{x}{2\nu_x} + \frac{y}{2\nu_y} + \omega\left(\frac{x}{2\nu_x} - \frac{y}{2\nu_y}\right), \tag{8}$$

where $\omega(\theta)$ is an arbitrary function of $\theta = [(x/2\nu_x) - (y/2\nu_y)]$.

Relationship (8) shows that the fractal exponents ν_x and ν_y contain only part of the information on the correlation properties of a fractal object. The rest of the information is contained in the function $\omega(\theta)$. Indeed, *Sapozhnikov and Foufoula-Georgiou* [1995, Figure 4] presented an example of fractal objects having the same values of ν_x and ν_y and different correlation properties because their $\omega(\theta)$ functions are different. It can be seen from (5) and (8) that while the fractal exponents ν_x and ν_y determine the direction of the generating line of the cylindric surface $z(x, y)$, the function $\omega(\theta)$ provides the additional information needed to describe the shape of any cross section of the cylindric surface. Thus together ν_x, ν_y, and $\omega(\theta)$ completely determine the shape of the logarithmic correlation integral surface $z(x, y)$.

By choosing the coordinate system (ξ, η, ζ), such that the (ξ, η) plane is perpendicular to the direction of the cylinder generating line, the surface $z(x, y)$ can be expressed as a function of one variable, $\eta(\xi)$, representing the curve of intersection of the cylinder with the (ξ, η) plane. *Sapozhnikov and Foufoula-Georgiou* [1995] showed that in this new coordinate system, the equation for the logarithmic correlation integral takes the form

$$\eta(\xi) = \frac{\nu_y^2 - \nu_x^2}{2\nu_x\nu_y\sqrt{1 + \nu_x^2 + \nu_y^2}}\xi + \frac{\sqrt{\nu_y^2 + \nu_x^2}}{\sqrt{1 + \nu_x^2 + \nu_y^2}}\omega\left(\frac{\sqrt{\nu_y^2 + \nu_x^2}}{2\nu_x\nu_y}\xi\right) \tag{9}$$

The function $\eta(\xi)$ is exactly what one sees viewing the $z(x, y)$ surface from the direction of the generating line. Since the (ξ, η) plane is orthogonal to the direction of the generating line, it is preferable to use $\eta(\xi)$ instead of $\omega(\theta)$ to describe the correlation properties of an object, since these properties are now not only complementary to the scaling exponents ν_x and ν_y (determining the direction of the generating line of the cylinder) but also independent of them.

It can be shown that the function $\omega(\theta)$ has two linear asymptotes at positive and negative infinities [see *Sapozhnikov and Foufoula-Georgiou*, 1995, p. 563]. This gives an important feature of the $z(x, y)$ surface, namely that, if large enough, it can be considered as composed of two asymptotic planes (see (14) and (15) below) and an intermediate zone between them. Also, it implies that $\eta'(\xi)$ has two asymptotic values, $\eta'(+\infty)$ and $\eta'(-\infty)$, which can be used to quantify the correlation characteristics of a self-affine object, other than the fractal exponents ν_x and ν_y. In particular, we introduce two parameters characterizing the correlation properties of self-affine objects: the "nonscaling anisotropy parameter" δ defined as

$$\delta \equiv [\eta'(-\infty) + \eta'(+\infty)]/2 \tag{10}$$

and the "curvature parameter" κ defined as

$$\kappa \equiv [\eta'(-\infty) - \eta'(+\infty)]/2 \tag{11}$$

These two parameters are important characteristics of a self-affine object and complement the information contained in the fractal exponents ν_x and ν_y. The value of δ characterizes the anisotropy of the cross section of the function $z(x, y)$. It is equal to zero when the cross section is isotropic and describes a different type of anisotropy of a self-affine object than the ratio of the scaling exponents ν_x/ν_y. In fact, *Sapozhnikov and Foufoula-Georgiou* [1995] showed that even a self-similar object ($\nu_x = \nu_y$) may have anisotropic correlation characteristics which are indicated by $\delta \neq 0$. To distinguish between these two types of anisotropy, we coined the terms "scaling anisotropy parameter" for ν_x/ν_y and "nonscaling anisotropy parameter" for δ. The parameter κ is a measure of curvature of $z(x, y)$. *Sapozhnikov and Foufoula-Georgiou* [1995] showed that if it is equal to zero, that is, the cylindric surface $z(x, y)$ degenerates into a plane, the exponents ν_x and ν_y of the fractal object are not defined uniquely.

3.3. Connection Between the Exponents ν_x and ν_y and Other Characteristics of Fractal Objects

Let D_{cx} and D_{cy} be the fractal dimensions of cross sections of the object in the directions of the x and y axes and D_{px2} and D_{py2} be the correlation fractal dimensions [see *Grassberger and Procaccia*, 1982] of the projections of the object on the x and y axes, respectively. Let us remind the reader that the generalized fractal dimensions D_q are

$$D_q = \lim_{\varepsilon \to 0} \frac{\log\left(\sum p_i^q\right)}{(q - 1)\log \varepsilon} \qquad q \neq 1 \tag{12}$$

$$D_1 = \lim_{\varepsilon \to 0} \frac{\sum p_i \log p_i}{\log \varepsilon}, \tag{13}$$

where p_i is the fraction of the measure in a box of size ε (in our case it is the fraction of the object that projects into an interval of size ε). D_0 is the fractal dimension of the support of the measure, and D_1 and D_2 are called information and correlation dimensions, respectively. Thus D_{px2} and D_{py2} are computed using (12) with $q = 2$ and with the p_i obtained using the projections of the object on the x and y axes.

Sapozhnikov and Foufoula-Georgiou [1995] showed the equations for the two asymptotic plane parts of the surface $z(x, y)$ to be

$$z_-(x, y) = D_{px2}x + D_{cy}y \tag{14}$$

$$z_+(x, y) = D_{cx}x + D_{py2}y \tag{15}$$

These relationships make it possible to demonstrate clearly what one gets when the fractal dimension of a self-affine object is determined: One finds how the mass within a $X \times Y$ rectangle changes as its sides change proportionally to each other. In other words, one just finds the slope of the section of the plane $z(x, y)$ by the plane $y = x + a$, where constant $a = \log(Y/X)$. If $\nu_x > \nu_y$, then for positive values of a ($Y > X$), the plane $y = x + a$ will intersect only the $z_-(x, y)$ plane, while for negative values of a, both $z_-(x, y)$ and $z_+(x, y)$ planes will be intersected. That creates two slopes, corresponding to what is called global and local fractal dimensions of a self-affine object D_G and D_L, correspondingly [*Mandelbrot*,

1986]. Putting $y = x + a$ in (14) and (15), we obtain that for $\nu_x > \nu_y$

$$D_G = D_{px2} + D_{cy} \tag{16}$$

$$D_L = D_{py2} + D_{cx} \tag{17}$$

It is easy to see from (14), (15), and (7) that *Mandelbrot*'s [1986] expressions

$$D_G = (\nu_y - \nu_x + 1)/\nu_y, \tag{18}$$

$$D_L = (\nu_x - \nu_y + 1)/\nu_x \tag{19}$$

can be obtained as a special case (for $D_{px2} = D_{py2} = 1$) of the more general expressions derived here.

Another set of useful relations, obtained from (7), (14), and (15), is

$$\nu_x D_{cx} + \nu_y D_{py2} = 1 \tag{20}$$

$$\nu_x D_{px2} + \nu_y D_{cy} = 1. \tag{21}$$

For example, these relationships can be used for estimation of ν_x and ν_y, given D_{cx}, D_{cy}, D_{px2}, and D_{py2}. Notice that for a self-similar object, (20) and (21) give

$$D_{cx} + D_{py2} = D_{cy} + D_{px2} = D \tag{22}$$

where D is the fractal dimension of the object.

4. Study of Spatial Scaling in Three Natural Rivers

As mentioned in the introduction, braided rivers manifest salient features of their spatial structure at scales below their width, where branching comes into play. Therefore we focused in this study on scales smaller than the braid plain width. The patterns of three rivers were analyzed: the Brahmaputra River (Bangladesh), the Aichilik River (Alaska), and the Hulahula River (Alaska). We used the traced air and satellite photo images of these rivers and tried to capture anabranches up to the smallest possible width. The tracing was done by a geologist experienced in morphology of braided rivers and their field observation (A. Brad Murray, Department of Geology and Geophysics, University of Minnesota). In the tracing, only active channels, that is, channels which are connected to the drainage system, were included. The traced photo images were then digitized to produce images consisting of black and white pixels indicating the presence or absence of active channels. The pixel size for each river was chosen such that the resolution of the digitized image was at least as good as the resolution of the traced photo, so that no details of the tracing were lost due to digitization.

The Brahmaputra is one of the world's largest rivers. It starts at Tibet and joins the Ganges near the Bay of Bengal. It is a very dynamic sand-bed river, with intensive bank erosion, mobile sand bars, less mobile islands, and frequent shifting of anabranches and switching flows between anabranches. The braid plain width of the Brahmaputra River reaches 20 km. The mean discharge is around 12,200 m^3/s. The hydrograph of the Brahmaputra River shows high annual variations, with lower flows in winter and high flows in summer (causing severe floods). Its highly dynamic nature causes a serious threat to the surrounding cities and villages and presents considerable problems for designers of bridges, roads, and other adjacent constructions. The river carries about 500 million tons of sediment annually, mostly silt and sand. Figure 2a shows the digitized image of the reach of the Brahmaputra River between Teesta and Ganges confluences, in winter stage.

The Aichilik and Hulahula Rivers are located at the North Slope of Alaska. The Aichilik is a gravel-bed river, with dominantly gravel to cobble-sized load. The gravel braid plain width is about 0.5 km. The river is fed largely by snow and permafrost melt. The Hulahula is a gravel-bed river, similar to the Aichilik except that it is a little larger (its braid plain is about 0.7 km) and largely glacially fed. The digitized photo images of the studied sections of the Aichilik and Hulahula Rivers are shown in Figures 2b and 2c, respectively. Some hydrologic and geomorphologic characteristics of the three rivers are summarized in Table 1. It can be seen from Table 1 that the rivers under study are characterized by large differences in their scales, slopes, and type of bed material. The braiding index (BI) for each river was computed as the average number of channels in cross sections of the photo image of the river (see *Bristow and Best* [1993] for several definitions of BI). Note that the BI is a resolution dependent quantity and therefore the BI values reported in Table 1, although properly reflecting the geometry of the analyzed images, are not directly comparable to each other due to the different resolution of the analyzed images. For example, in the case of the Brahmaputra River the computed BI value is lower than its actual value since the sizes of the smallest existing channels are below the resolution of the photo used in this analysis.

First, a traditional fractal analysis was applied. Square boxes of size R were positioned around every black pixel (i.e., every pixel indicating the presence of active channels), and the average number of black pixels within squares of size R was computed. The "mass" $M(R)$ was then calculated by multiplying this average number of pixels by the area of a pixel. Figures 3a, 3b, and 3c present in log-log scale the dependence of M on R for the Brahmaputra, Aichilik, and Hulahula Rivers, respectively. For the Brahmaputra River the dependence follows a straight line up to the scale of 15 km, and the slope of the line is 1.50. For the Aichilik and Hulahula Rivers, scaling is observed up to scales of 0.5 km and 0.7 km, respectively, and the slopes of the best fit straight lines are 1.58 and 1.54, respectively. One can see that for all three rivers, the upper scale of linearity of these lines coincides with the rivers' width shown in Table 1. The estimated values of the fractal dimensions agree with the results of *Nikora et al.* [1995], who found fractal dimension $D = 1.5$–1.7 for several New Zealand braided rivers using a box-counting method (number of cells containing the pattern as a function of the grid cell size). However, the linear (in log-log scale) $M(R)$ dependence itself does not show whether the object is self-similar or self-affine. Indeed, self-affine objects can still show linear log-log dependence of $M(R)$. As demonstrated in section 3 (see (14) and (15) and discussion afterward) the $M(R)$ dependence may have either two slopes at different scales (D_L at smaller scale and D_G at bigger scale) or one slope D_G. For example, in the case of the biased random walk considered in section 2, if the steps in the X direction have the same length as the steps in the Y direction, one obtains just one trivial fractal dimension $D_G = 1$ which obviously does not reflect fully the scaling properties of this self-affine object expressed by the fractal exponents $\nu_x = 1$, $\nu_y = 1/2$.

To find the fractal exponents of the braided rivers under investigation, we first estimated their logarithmic correlation integrals $z(x, y)$ from the patterns of the rivers. The x axis was

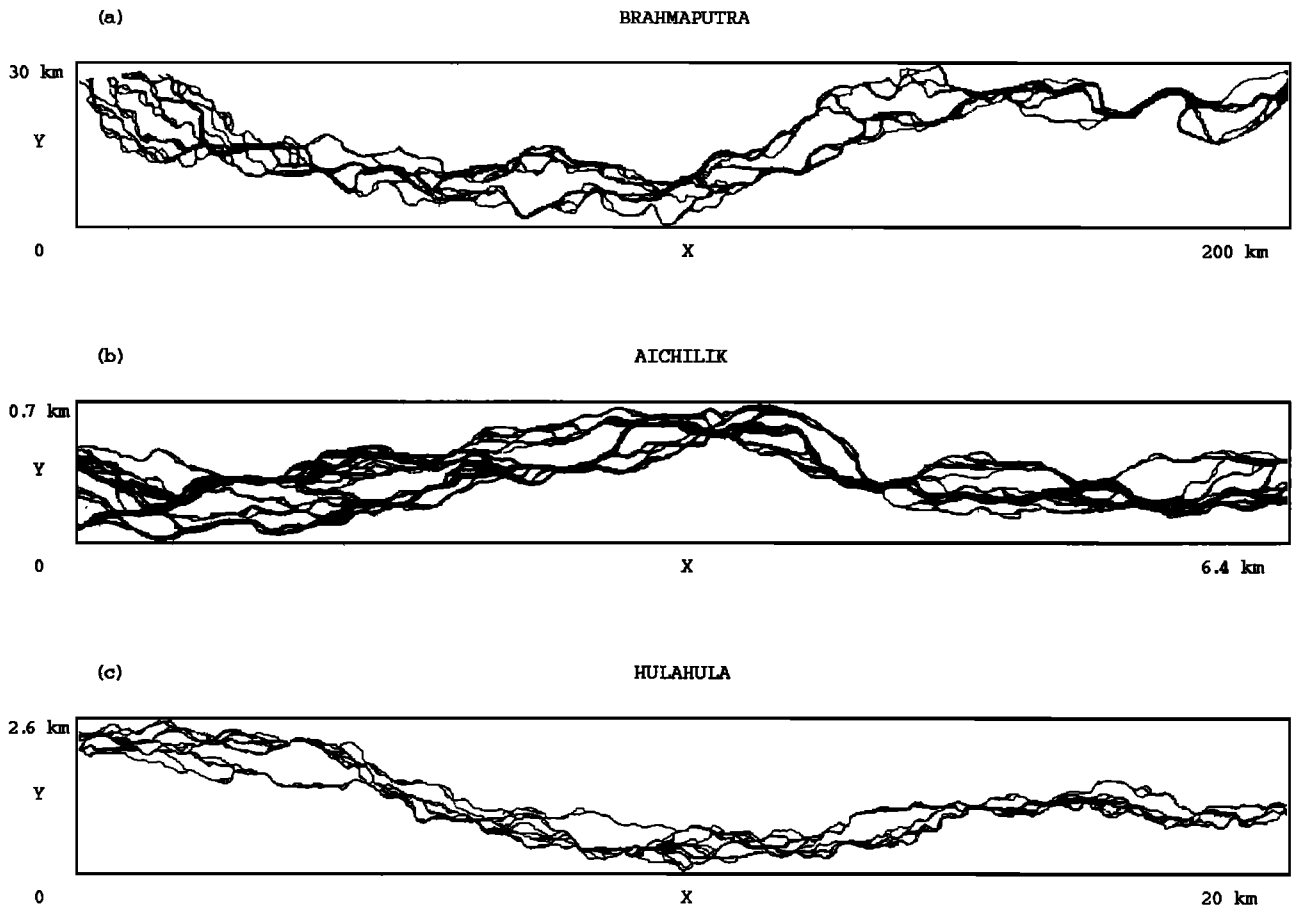

Figure 2. The digitized images of (a) the Brahmaputra River (Bangladesh), (b) the Aichilik River (Alaska), and (c) the Hulahula River (Alaska).

oriented along the line connecting the beginning and the end of the analyzed section of each river. The $z(x, y)$ surface for the Brahmaputra River is presented in Figure 4; the surfaces for the other two rivers look similar and are not shown here. From the correlation integral surfaces $z(x, y)$ we calculated numerically the derivatives $\partial z(x, y)/\partial x$ and $\partial z(x, y)/\partial y$ and plotted the dependence $\partial z(x, y)/\partial y$ versus $\partial z(x, y)/\partial x$. The dependence for the Brahmaputra River is presented in Figure 5a. According to (7), in the self-affinity region the partial derivatives should show linear dependence. However, one can see that while the upper part of the plot in Figure 5a shows linearity, the dependence breaks in the lower part of the plot. It is natural to expect that there is a scaling break at a certain scale, namely for Y values bigger than the average width of the river (approximately 15 km). This scaling break is also reflected in Figure 3a, showing deviation from the straight line for scales greater than 15 km. To check if the points in the lower part of the plot come from this range of scales, we cut off the part of the $z(x, y)$ surface corresponding to the Y values higher than 15 km (see Figure 6 for the truncated $z(x, y)$ surface of the Brahmaputra River). Figure 7a displays the values of the partial derivatives coming from the part of the correlation integral shown in Figure 6. The points show a good linear dependence, indicating that this part of the $z(x, y)$ surface is cylindric; that is, the Brahmaputra River exhibits spatial scaling within the examined scales of Y (0.4–15 km: the width of the smallest included channels to braid plain width). Using (7) we calculated the values of the fractal exponents for the Brahmaputra River. They are $\nu_x = 0.74$ and $\nu_y = 0.51$. Similar analysis applied to the Aichilik and Hulahula Rivers

Table 1. Hydrologic and Geomorphologic Characteristics of the Studied Rivers

	Brahmaputra	Aichilik	Hulahula
Reach width, km	15	0.5	0.7
Reach length, km	200	6.4	20
Mean channel depth, m	5	1	1
Slope	0.000077	0.001	0.0007
Braiding index*	3.8	6.8	5.2
Predominant type of the bed material	sand	gravel	gravel

*The braiding index (BI) for each river was computed as the average number of channels in cross sections of the photo image of the river (see section 4 for more discussion).

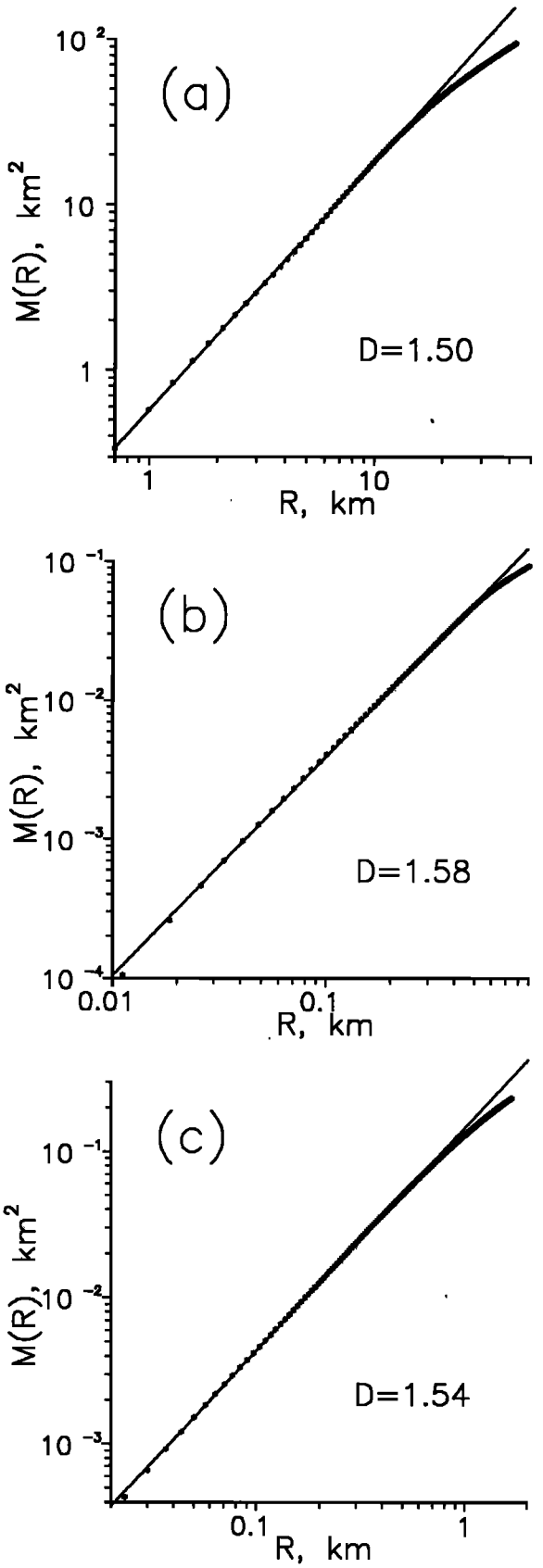

Figure 3. Spatial scaling in the (a) Brahmaputra, (b) Aichilik, and (c) Hulahula Rivers indicated by straight-line log-log dependence of the "mass" M on the size of the square box R (see text for the definition). The slopes of the straight lines give the values of the fractal dimensions D.

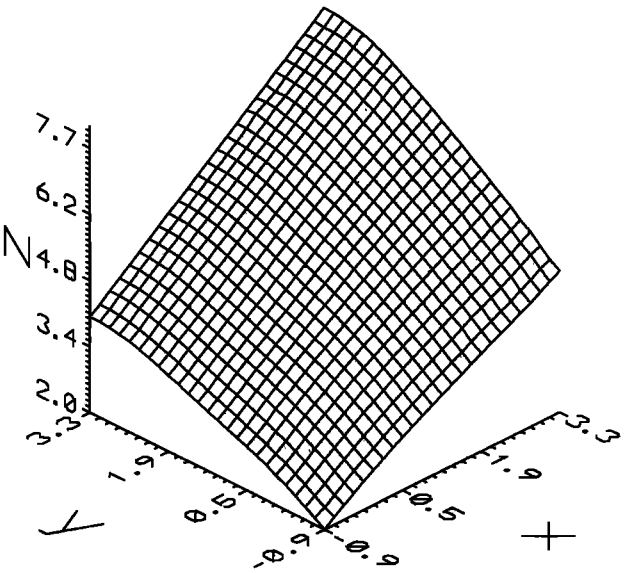

Figure 4. Logarithmic correlation integral surface $z(x, y)$ of the Brahmaputra River.

(Figures 5b, 5c, 7b, and 7c) gave fractal exponents $\nu_x = 0.72$, $\nu_y = 0.51$ and $\nu_x = 0.74$, $\nu_y = 0.52$, respectively. These results imply that all three rivers are self-affine objects showing a rather high degree of anisotropy: $\nu_x/\nu_y = 1.45$ for the Brahmaputra, $\nu_x/\nu_y = 1.41$ for the Aichilik, and $\nu_x/\nu_y = 1.42$ for the Hulahula. The values of the fractal exponents ν_x and ν_y agree with the results of the traditional fractal analysis shown in Figures 3a, 3b, and 3c ("mass" within a box as a function of the box size) which is expected to show a slope equal to the value of the global fractal dimension D_G for a self-affine object. Indeed, for the estimated values of ν_x and ν_y the global fractal dimensions according to *Mandelbrot* [1986] (see also (18) here) are found to be $D_G = 1.51$ for the Brahmaputra, $D_G = 1.55$ for the Aichilik, and $D_G = 1.50$ for the Hulahula. These values are very close to the corresponding values of D obtained previously from the slopes of $M(R)$ log-log linear dependence (1.50, 1.58, and 1.54, respectively). The results of the analysis are summarized in Table 2.

Since the function $z(x, y)$ of a fractal object is a cylindric surface it can be viewed in the direction of the cylinder generating line (see (5) and (6)). In other words, it is possible to adjust the rotation angle φ about the z axis and the tile angle ψ above the (x, y) plane from which the surface is viewed to see only the edge of the surface (which is the $\eta(\xi)$ function of (9)). It is not difficult to show that the following relationships connecting the angles and the exponents hold

$$\tan \varphi = \nu_x/\nu_y \tag{23}$$

$$\sin \psi = (1 + \nu_x^2 + \nu_y^2)^{-1/2}. \tag{24}$$

Figure 8 shows the $z(x, y)$ surface of the Brahmaputra River viewed from the angles $\varphi = 36.6°$ and $\psi = 47.7°$ determined by (23) and (24). It can be seen that $z(x, y)$ really represents a cylindric surface and that the angles φ and ψ correspond to relationships (23) and (24). What one sees in Figure 8 is a cross section of the cylindric surface $z(x, y)$ by a plane perpendicular to the cylinder generating line; that is, one sees the $\eta(\xi)$ function (9). By the same procedure we rotated the $z(x, y)$

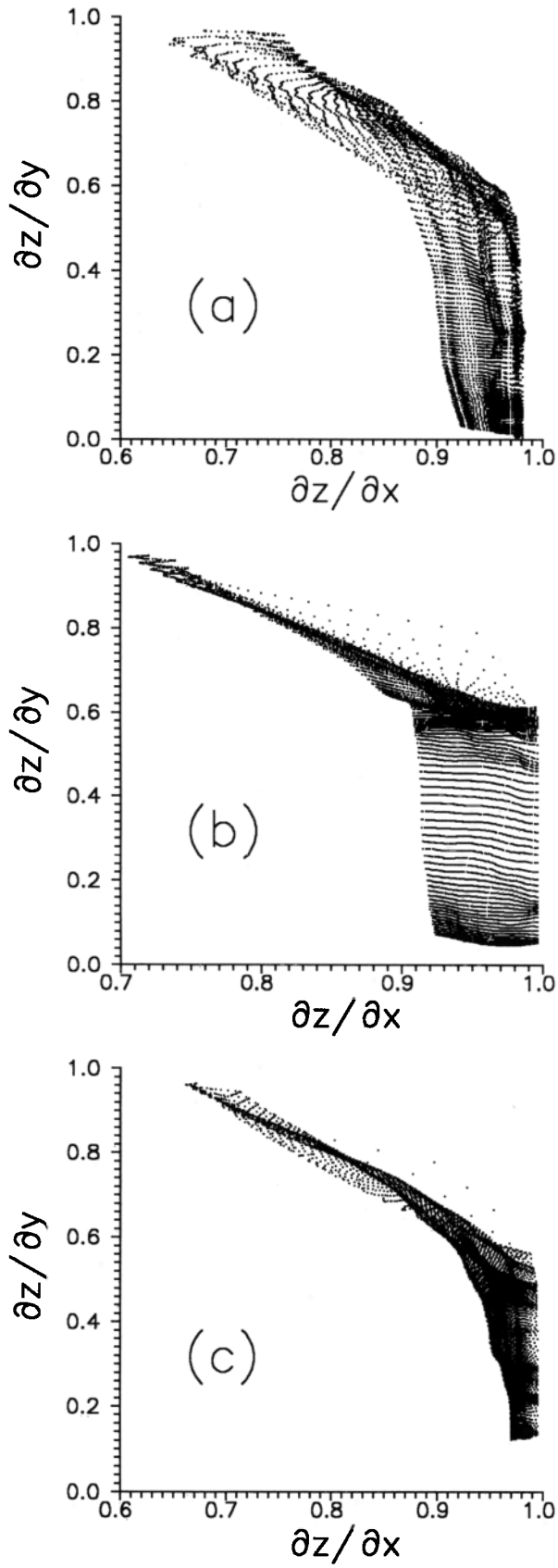

Figure 5. Dependence $\partial z(x, y)/\partial y$ versus $\partial z(x, y)/\partial x$ for the (a) Brahmaputra, (b) Aichilik, and (c) Hulahula Rivers. The partial derivatives are estimated from the entire correlation integral surfaces $z(x, y)$ of the rivers (see Figure 4 for the $z(x, y)$ surface of the Brahmaputra).

surfaces of the Aichilik and Hulahula Rivers at the appropriate φ and ψ angles and found that they look similar to the rotated $z(x, y)$ surface of the Brahmaputra River shown in Figure 8.

As we already stated, the $z(x, y)$ surface of a self-affine object asymptotically approaches two planes (one when $x/2\nu_x - y/2\nu_y$ is a large positive value and the other when it is a large negative value). Therefore, if the $z(x, y)$ surface is large enough to reach its asymptotic behavior, one can think of it as being composed of two planes and an intermediate zone between them. The analysis of the $z(x, y)$ functions of all three rivers shows that they do not reach their asymptotic behavior within the studied region; that is, we deal only with the intermediate zone in this case. This did not allow us to estimate reliably the values of D_{cx}, D_{cy}, D_{px2}, D_{py2}, and accordingly, the anisotropy parameter δ and curvature parameter κ. Rough estimates show that they are both of the order of 0.1, i.e., small values, which implies that the $z(x, y)$ surfaces are not inclined significantly to the x or y axes (indicating that there is no significant nonscaling anisotropy in the patterns of the analyzed rivers) and are not very curved.

5. Robustness of Scaling Exponent Estimates

In studying a natural river for self-affine scaling with the proposed method, there are three sources of subjectivity (and therefore uncertainty) which can potentially affect the obtained estimates of fractal exponents. The first source of subjectivity relates to the procedure of tracing the river image from an aerial photograph, the second relates to the selection of the orientation of the coordinate axes, and the third relates to the choice of the portion of the $z(x, y)$ surface used for estimation of the fractal exponents ν_x and ν_y. The sensitivity of the obtained estimates to these three factors gives an indication of the robustness of the proposed method in estimating the self-affine structure of a natural braided river.

In tracing the river image from an aerial photograph one must decide whether or not to include small channels that are on the threshold of vision. To test the sensitivity of the esti-

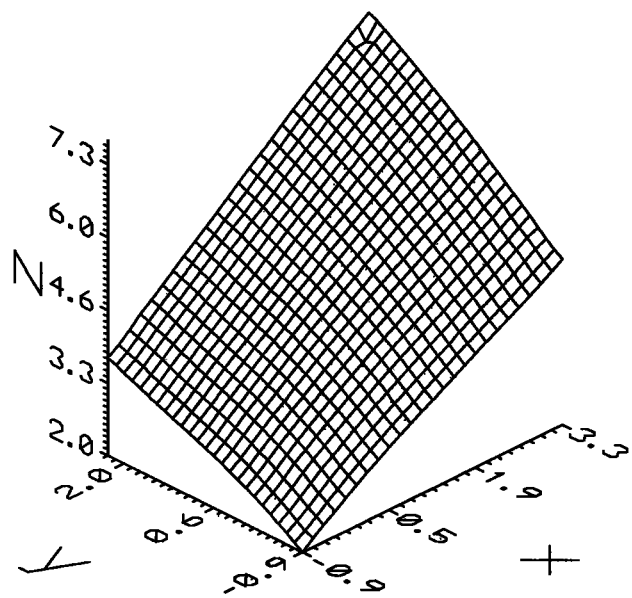

Figure 6. Truncated logarithmic correlation integral surface $z(x, y)$ of the Brahmaputra River.

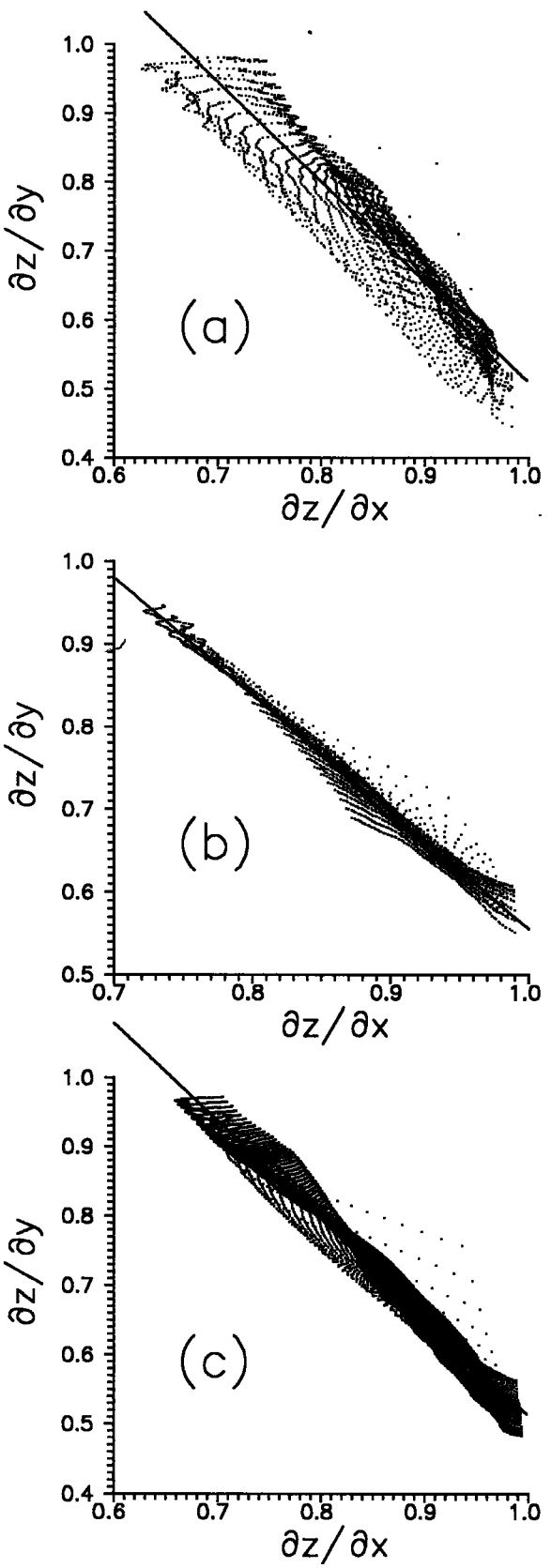

Figure 7. Estimation of the fractal exponents ν_x and ν_y for the (a) Brahmaputra, (b) Aichilik, and (c) Hulahula Rivers from the truncated parts of the $z(x, y)$ surfaces (see Figures 6 and 8). Advantage is taken of (7). The estimated values are $\nu_x = 0.74$, $\nu_y = 0.51$ for Figure 7a, $\nu_x = 0.72$, $\nu_y = 0.51$ for Figure 7b, and $\nu_x = 0.74$, $\nu_y = 0.52$ for Figure 7c.

Table 2. Fractal Characteristics of the Studied Rivers

River	ν_x	ν_y	ν_x/ν_y	D_G, (18)	D, (2)
Brahmaputra	0.74	0.51	1.45	1.51	1.50
Aichilik	0.72	0.51	1.41	1.55	1.58
Hulahula	0.74	0.52	1.42	1.50	1.54

mated values of fractal exponents ν_x and ν_y to the tracing procedure, we analyzed two tracings of the same aerial photograph of the Aichilik River. The first tracing, for which the results were reported in the previous section, included all visible channels, while the second tracing did not include the smallest, and therefore questionable, channels. The estimated values of the fractal exponents for the second tracing were $\nu_x = 0.78$ and $\nu_y = 0.55$, not very different from the corresponding exponents of the tracing which included all small channels ($\nu_x = 0.72$ and $\nu_y = 0.51$). The anisotropy parameter $\nu_x/\nu_y = 1.42$ was practically the same as in the first tracing ($\nu_x/\nu_y = 1.41$). Quite naturally, for this tracing, because of absence of small details, the scaling breaks at small scales, so that up to the width of the smallest included channels (25 m) the $M(R)$ dependence has a slope close to 2. For the same reason the $z(x, y)$ surface of this tracing also deviated from a cylindric surface up to the scales of 15 m. This observation suggests that the self-affinity of braided rivers, observed up to the rivers' width, starts at the scales of the width of the smallest channels.

In our analysis the coordinate system was oriented such that the x axis is directed along the line connecting the endpoints of the analyzed section of the river. However, because this coordinate system depends on the analyzed segment of the river, the sensitivity of the obtained estimates to the orientation of the coordinates system was tested. For that we rotated the coordinate system in the Brahmaputra River by 8° counterclockwise. This value corresponds to deviation of the x axis from one of the endpoints of the analyzed section by approximately two widths of the river. This rotation changed the

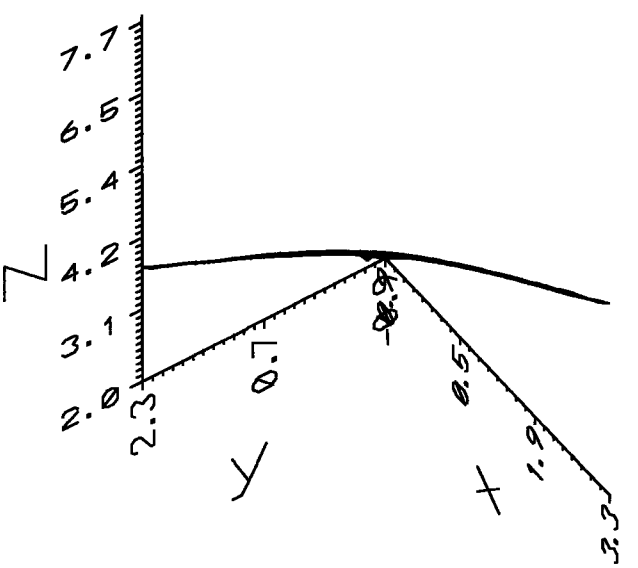

Figure 8. Truncated logarithmic correlation integral surface $z(x, y)$ of the Brahmaputra River viewed from the direction of the cylinder generating line (see (23) and (24)).

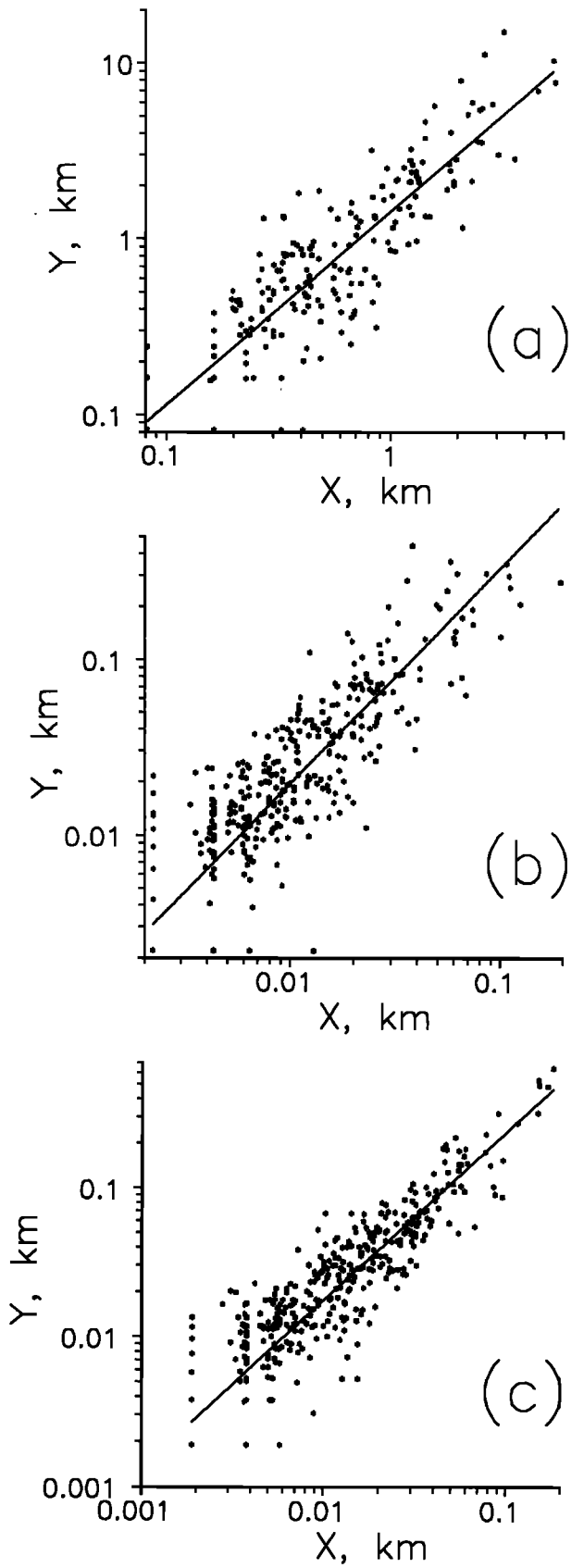

Figure 9. Scaling in the projections of the islands on the x and y axes. The slopes are different from 1, indicating scaling anisotropy. The estimated values of the slopes are (a) 1.2 for the Brahmaputra, (b) 1.3 for the Aichilik, and (c) 1.2 for the Hulahula.

Table 3. Average Fractal Characteristics of Single-Channel Rivers, River Networks, and Braided Rivers

Objects	ν_x	ν_y	ν_x/ν_y	D_G, (18)
Single-channel rivers*	~1	~0.5	~2	~1
River networks†	0.62	0.47	1.32	1.83
Braided rivers‡	0.73	0.51	1.43	1.52

*Reaches of the Dniester and Pruth Rivers in Moldova [*Nikora et al.*, 1993].
†Sixty river networks [*Nikora and Sapozhnikov*, 1993; *Nikora*, 1994].
‡This study.

values of the fractal exponents only slightly from $\nu_x = 0.74$, $\nu_y = 0.51$ to $\nu_x = 0.73$, $\nu_y = 0.54$. Naturally, since we artificially deviated from the real direction of the river, the anisotropy in spatial scaling decreased somewhat (from $\nu_x/\nu_y = 1.45$ for the initial picture to $\nu_x/\nu_y = 1.35$ for the rotated one).

Another element of subjectivity comes from choosing the portion of the logarithmic correlation integral surface $z(x, y)$ for estimating the self-affine characteristics of the object. This problem is similar to that of choosing the portion of the log-log $M(R)$ plot for straight-line fit in a traditional fractal analysis (see Figures 3a, 3b, and 3c). The choice of the portion of the $z(x, y)$ surface affects the estimated values of the fractal exponents. We tested our method by selecting different portions of the $z(x, y)$ surface for analysis (see Figures 6 and 8) and then calculating the fractal exponents for each. The test gave the following small ranges of the fractal exponents: for the Brahmaputra River, $\nu_x = 0.73$–0.75 and $\nu_y = 0.51$–0.55; for the Aichilik River, $\nu_x = 0.71$–0.74 and $\nu_y = 0.50$–0.52; for the Hulahula River, $\nu_x = 0.71$–0.75 and $\nu_y = 0.50$–0.54.

The results of these tests indicate that our method for analyzing and estimating scaling in self-affine natural objects is reasonably robust. However, one cannot expect it to be as robust as traditional fractal analysis because it reveals subtler features of spatial scaling of the objects.

6. Scaling in the Sizes of Islands

As another indicator of scaling anisotropy we also studied sizes of islands (here we did not distinguish between islands and exposed bars surrounded by water). The log-log plots of the projections of the islands on the x and y axes, ΔX and ΔY, respectively, displayed in Figures 9a, 9b, and 9c, reveal scaling. The slopes are different from 1, indicating anisotropy in scaling of the islands in X and Y directions. The slopes of these plots are 1.2 for the Brahmaputra, 1.3 for the Aichilik, and 1.2 for the Hulahula. They are lower than the obtained values of the scaling anisotropy parameters for the rivers, ν_x/ν_y, which were equal to 1.45, 1.41, and 1.42, respectively. In our opinion this difference implies that the scaling anisotropy of a braided river is only partially reflected by the anisotropy of islands; part of the anisotropy in a braided river stems from the anisotropy in tortuosity of the river (same as anisotropy in tortuosity of single-channel rivers causing their scaling anisotropy). These two factors exist on scales which overlap and therefore cannot be separated. The relations between scaling anisotropy in size distribution of islands and fractal structure of a braided river need further study, which is outside the scope of the present article.

7. Concluding Remarks

Within the scales of their width the three studied rivers (the Brahmaputra in Bangladesh and the Aichilik and Hulahula in Alaska) are self-affine, with fractal exponents $\nu_x = 0.72–0.74$ and $\nu_y = 0.51–0.52$. Table 3 enables one to compare these fractal exponents with the fractal exponents of other self-affine hydrologic objects. In Table 3 the average fractal characteristics of the analyzed braided rivers are listed together with the average fractal characteristics (in the self-affinity regions) of single-channel rivers Dniester and Pruth [*Nikora et al.*, 1993] and of 60 river networks [*Nikora and Sapozhnikov*, 1993; *Nikora*, 1994]. Comparison of the fractal characteristics of the hydrologic objects summarized in Table 3 suggests a conclusion that braided rivers form a class of fractal objects which lies between the classes of single-channel rivers and river networks. Indeed, the scaling anisotropy of braided rivers (characterized by the ν_x/ν_y value) is lower than that of single-channel rivers but higher than that of river networks; the global fractal dimension D_G shows that braided rivers fill the surface more densely than single-channel rivers but not as densely as river networks. It should be noticed that in contrast to the single-channel rivers, no self-similarity range of scales was revealed in the studied braided rivers. In our opinion the absence of the self-similarity region in braided rivers is related to the lower sinuosity of their channels [see *Friend and Sinha*, 1993, p. 110].

The fact that despite big difference in scales, slopes, and types of bed material (see Table 1) the analyzed braided rivers show similar spatial scaling is worthy of notice. It might indicate that the spatial structure of braided rivers is determined by universal physical mechanisms. However, more braided rivers need to be studied to validate this hypothesis.

The study of the fractal geometry of braided rivers and scaling in their hydrologic characteristics can eventually help to relate their geometry to the hydrologic characteristics and dynamics of the rivers, as it was partially done for individual streams and river networks. This is a challenging area of research which we are currently pursuing with the help of experimentally produced braided rivers in our laboratory.

Acknowledgments. This research was partially supported by NSF grant BSC-8957469 and NASA grant NAG-52108. Supercomputer resources were kindly provided by the Minnesota Supercomputer Institute. The aerial photographs for the Aichilik and Hulahula Rivers were provided to us by Chris Paola's group at the Department of Geology and Geophysics, University of Minnesota, and the tracing was performed by A. Brad Murray. Without their help this study would not have been possible.

References

Bristow, C., and J. Best, Braided rivers: Perspectives and problems, in *Braided Rivers*, edited by J. Best and C. Bristow, pp. 1–11, Geol. Soc., London, 1993.

Friend, P. F., and R. Sinha, Braiding and meandering parameters, in *Braided Rivers*, edited by J. Best and C. Bristow, pp. 105–111, Geol. Soc., London, 1993.

Grassberger, P., and I. Procaccia, Measuring of strangeness of strange attractors, *Physica D*, *9*, 189–208, 1982.

Howard, A. D., M. E. Keetch, and C. L. Vincent, Topological and geometrical properties of braided streams, *Water Resour. Res.*, *6*, 1674–1688, 1970.

Ijjasz-Vasquez, E. I., R. Bras, and I. Rodriguez-Iturbe, Self-affine scaling of fractal river courses and basin boundaries, *Physica A*, *209*, 288–300, 1994.

Kondoh, H., M. Matsushita, and Y. Fukuda, Self-affinity of Scheidegger's river patterns, *J. Phys. Soc. Jpn.*, *56*, 1913–1915, 1987.

La Barbera, P., and R. Rosso, On the fractal dimension of stream networks, *Water Resour. Res.*, *25*, 735–741, 1989.

Lane, E., *A Study of the Shape of Channels Formed by Natural Streams Flowing in Erodable Material, M.R.D. Sediment Ser.*, vol. 9, U.S. Army Eng. Div., Mo. River, Corps Eng., Omaha, Neb., 1957.

Mandelbrot, B. B., *The Fractal Geometry of Nature*, W. H. Freeman, New York, 1982.

Mandelbrot, B. B., Self-affine fractal sets, in *Fractals in Physics, Proceedings of the Sixth Trieste International Symposium on Fractals in Physics, ICTP, Trieste, Italy*, edited by L. Petroniero and E. Tosatti, pp. 3–16, North-Holland, New York, 1986.

Matsushita, M., and S. Ouchi, On the self-affinity of various curves, *Physica D*, *38*, 246–251, 1989.

Meakin, P., J. Feder, and T. Jossang, Simple statistical models for river networks, *Physica A*, *176*, 409–429, 1991.

Murray, A. B., Braided-stream modeling and model evaluation: Dynamical-systems approaches, Ph.D. thesis, Univ. of Minnesota, Minneapolis, 1995.

Murray, A. B., and C. Paola, A cellular automata model of braided rivers, *Nature*, *371*, 54–57, 1994.

Murray, A. B., and C. Paola, A new quantitative test of geomorphic models, applied to a model of braided streams, *Water Resour. Res.*, in press, 1996.

Nikora, V. I., Fractal structures of river plan forms, *Water Resour. Res.*, *27*, 1327–1333, 1991.

Nikora, V. I., On self-similarity and self-affinity of drainage basins, *Water Resour. Res.*, *30*, 133–137, 1994.

Nikora, V. I., and V. B. Sapozhnikov, River network fractal geometry and its computer simulation, *Water Resour. Res.*, *29*, 3569–3575, 1993.

Nikora, V. I., V. B. Sapozhnikov, and D. A. Noever, Fractal geometry of individual river channels and its computer simulation, *Water Resour. Res.*, *29*, 3561–3568, 1993.

Nikora, V. I., D. M. Hicks, G. M. Smart, and D. A. Noever, Some fractal properties of braided rivers, paper presented at the 2nd International Symposium on Fractals and Dynamic Systems in Geoscience, Johann Wolfgang Goethe Univ., Frankfurt/Main, Germany, April 4–7, 1995.

Peckham, S. D., New results for self-similar trees with application to river networks, *Water Resour. Res.*, *31*, 1023–1029, 1995.

Rodriguez-Iturbe, I., E. Ijjasz-Vasquez, R. Bras, and D. Tarboton, Power law distributions of discharge mass and energy in river basins, *Water Resour. Res.*, *28*, 1089–1093, 1992.

Sapozhnikov, V. B., and E. Foufoula-Georgiou, Study of self-similar and self-affine objects using logarithmic correlation integral, *J. Phys. A Math. Gen.*, *28*, 559–571, 1995.

Sapozhnikov, V. B., and V. I. Nikora, Simple computer model of a fractal river network with fractal individual watercourses, *J. Phys. A Math. Gen.*, *26*, L623–L627, 1993.

Tarboton, D. G., R. L. Bras, and I. Rodriguez-Iturbe, The fractal nature of river networks, *Water Resour. Res.*, *24*, 1317–1322, 1988.

Webb, E. K., Simulation of braided channel topology and topography, *Water Resour. Res.*, *31*, 2603–2611, 1995.

E. Foufoula-Georgiou and V. Sapozhnikov, St. Anthony Falls Laboratory, University of Minnesota, Mississippi River at Third Avenue S.E., Minneapolis, MN 55414. (e-mail: sapoz001@maroon.tc.umn.edu)

(Received July 24, 1995; revised February 6, 1996; accepted February 8, 1996.)